Effect of Apex Angle on Absorption Characteristic of Pyramidal Absorbers

***Sedef Kent*[1], *Ibrahim Catalkaya*[2]**

[1] Istanbul Technical University, Electrical and Electronic Engineering Faculty, Electronics and Communication Engineering Department, Maslak, Istanbul, 34469, Turkey, kents@itu.edu.tr

[2] Istanbul Technical University, Vocational School, Technical Programs Department, Maslak, Istanbul, 34469, Turkey, catalkaya@itu.edu.tr

Abstract

Array of absorbing pyramid cones are widely used in anechoic chambers to measure electromagnetic wave interference Accuracy of measurements is related with absorbing performance of pyramidal structures on chamber walls. Absorbing performance of pyramidal structure depends on various parameters such as dielectric permittivity, magnetic permeability, material used for pyramids, physical dimensions of absorber etc. To determine effect of apex angle on absorption characteristics, absorbers which have different apex angles with same material are investigated. Reflectivity values are calculated. Both normal and oblique incidences of plane wave are analyzed. Results for different incidences angles and frequency bands are presented.

Keywords: Anechoic chamber; Electromagnetic wave interference; Apex angle; Absorption characteristic of pyramidal absorber.

1. Introduction

Pyramidal absorbers are widely used in anechoic chambers for the measurement of the electromagnetic wave interference. Absorption characteristic of them depends on their dimensions and dielectric properties in the given frequency band. Main purposes of researches are developing absorbers which have better low normal incidence reflection, low forward scattering and backscattering at wide incidence angle range, and reducing absorber height to use chamber space efficiently [1]. Pyramid geometry gave rise to multiple reflections in the direction of the pyramid apex. This facility was put to practical measurement use by the M. I. T. Radiation Laboratory [2]. Pyramidal absorber patented by Leland K. Neher in 1945 and he chose apex angle around 40° [3].

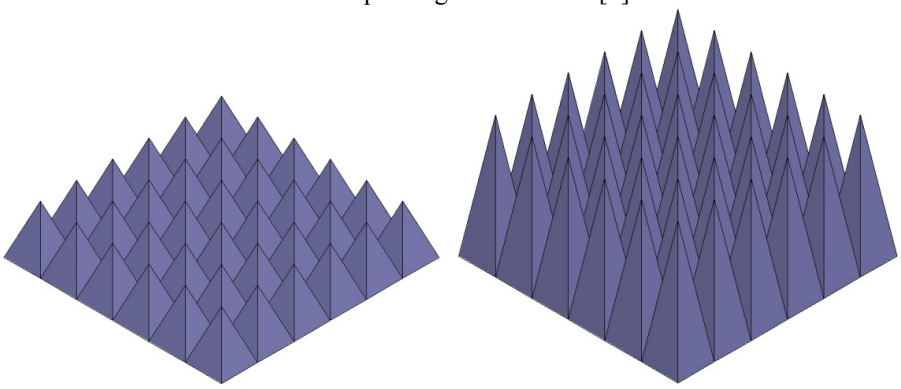

Figure 1. Pyramidal arrays with different apex angles and heights while same base length a) Pyramidal array with 40˚ apex angle b) Pyramidal array with 20˚ apex angle

Since the size of individual pyramids are relatively large compared to a wavelength of incident plane wave, surfaces of pyramids reflect the incident wave. After reflection many times between adjacent pyramids surfaces, the wave is highly attenuated. Upon each reflection, a portion of the wave's energy is absorbed by the lossy material of the pyramids. Amount of the absorbed energy is depends on reflection coefficient of the dielectric material (total reflection coefficient will be lower with more reflections). An extremely small portion of the incident wave can reach the metal back plate of the absorber array with multiple reflections [4]. Some portion of the incidence wave travels away from the pyramid array after several reflections. Reflection number of incident wave is depends on apex angle of the pyramids and incidence angle of the plane wave.

978-1-4244-6051-9/11/$26.00 ©2011 IEEE

Here, we analyzed effect of apex angle value of a pyramid absorber on reflection coefficient. It can be explained easily by using reflection coefficient calculation for normal and oblique incidence at a plane lossy dielectric boundary of plane wave theory and Snell's law of reflection. Since period of the array is relatively large compared with a wavelength, ray optics techniques can be used.

2. Theory

When the wavelength is small compared to significant dimensions of the objects, ray optics is applicable for incidence of electromagnetic wave to the objects [5].

Oblique incidence case of a uniform plane wave on a plane interface between two dielectric media (medium 2 is lossy for this case) can be used to explain reflection and transmission. Some portion of plane wave is reflected and other portion is transmitted. Reflection and refraction angles can be calculated easily by using Snell's law of reflection and refraction. Reflection and transmission coefficient can also be calculated. This well-known subject is explained below by using Cheng's study [6]. Let consider boundary between two media is $z = 0$, for perpendicular polarization case, the incidence electric and magnetic field intensity phasors in medium 1 are,

$$\mathbf{E}_i(x,z) = \boldsymbol{a}_y E_{i0} e^{-j\beta_1(xsin\theta_i + zcos\theta_i)} \tag{1}$$

$$\mathbf{H}_i(x,z) = \frac{E_{i0}}{\eta_1}(-\boldsymbol{a}_x cos\theta_i + \boldsymbol{a}_z sin\theta_i) e^{-j\beta_1(xsin\theta_i + zcos\theta_i)} \tag{2}$$

the reflected electric and magnetic fields are,

$$\mathbf{E}_r(x,z) = \boldsymbol{a}_y E_{r0} e^{-j\beta_1(xsin\theta_i - zcos\theta_i)} \tag{3}$$

$$\mathbf{H}_r(x,z) = \frac{E_{r0}}{\eta_1}(\boldsymbol{a}_x cos\theta_r + \boldsymbol{a}_z sin\theta_r) e^{-j\beta_1(xsin\theta_r - zcos\theta_r)} \tag{4}$$

in medium 2 the transmitted electric and magnetic field intensity phasors are,

$$\mathbf{E}_t(x,z) = \boldsymbol{a}_y E_{t0} e^{-\gamma_2(xsin\theta_t + zcos\theta_t)} \tag{5}$$

$$\mathbf{H}_t(x,z) = \frac{E_{t0}}{\eta_2}(-\boldsymbol{a}_x cos\theta_t + \boldsymbol{a}_z sin\theta_t) e^{-\gamma_2(xsin\theta_t + zcos\theta_t)} \tag{6}$$

from the requirements that the tangential components of **E** and **H** be continuous at the boundary $z = 0$. From $E_{iy}(x,0) + E_{ry}(x,0) = E_{ty}(x,0)$ and $H_{ix}(x,0) + H_{rx}(x,0) = H_{tx}(x,0)$ we have,

$$E_{i0} e^{-j\beta_1 xsin\theta_i} + E_{r0} e^{-j\beta_1 xsin\theta_r} = E_{t0} e^{-\gamma_2 xsin\theta_t} \tag{7}$$

$$\frac{1}{\eta_1}(-E_{i0} cos\theta_i e^{-j\beta_1 xsin\theta_i} + E_{r0} cos\theta_r e^{-j\beta_1 xsin\theta_r}) = -\frac{E_{t0}}{\eta_2} cos\theta_t e^{-\gamma_2 xsin\theta_t} \tag{8}$$

from phase matching, we can write $E_{i0} + E_{r0} = E_{t0}$ and $\frac{1}{\eta_1}(E_{i0} - E_{r0}) cos\theta_i = \frac{E_{t0}}{\eta_2} cos\theta_t$. We have,

$$\Gamma_\perp = \frac{\eta_2 cos\theta_i - \eta_1 cos\theta_t}{\eta_2 cos\theta_i + \eta_1 cos\theta_t} \tag{9}$$

for the parallel polarization case, the incidence electric and magnetic field intensity phasors in medium 1 are,

$$\mathbf{E}_i(x,z) = E_{i0}(\boldsymbol{a}_x cos\theta_i - \boldsymbol{a}_z sin\theta_i) e^{-j\beta_1(xsin\theta_i + zcos\theta_i)} \tag{10}$$

$$\mathbf{H}_i(x,z) = \boldsymbol{a}_y \frac{E_{i0}}{\eta_1}_x e^{-j\beta_1(xsin\theta_i + zcos\theta_i)} \tag{11}$$

similarly to the perpendicular polarization case, from the requirements that the tangential components of **E** and **H** be continuous at the boundary z=0, reflection coefficient can be written as,

$$\Gamma_{\parallel} = \frac{\eta_2 cos\theta_t - \eta_1 cos\theta_i}{\eta_2 cos\theta_t + \eta_1 cos\theta_i} \tag{12}$$

in general, total reflection coefficient will be,

$$\Gamma = \Gamma_1 . \Gamma_2 . \Gamma_3 \ldots . \Gamma_n \tag{13}$$

where Γ_i is *i*-th reflection coefficient, *i=1,2,3,….,n.*

3. Simulation Results

In this section, several simulation results are presented for different pyramidal absorbers arrays which have different apex angles. They are analyzed by using well known commercial simulator, Ansoft's HFFS software v12.1. HFFS utilizes a 3D full wave finite element method to compute the electrical behavior of high frequency components. Results are obtained for different apex angles of pyramidal arrays and different incidence angles of plane electromagnetic waves. %26 carbon loaded urethane is used as material which has relative dielectric permittivity ε=2.01+1.17*i* for 1000 MHz [4]. Magnetic permeability is $\mu = \mu_0 = 4\pi 10^{-7}$.H/m for the material. Base length of pyramids is $L=2\lambda$ which is suitable for ray optic approximation. Height of pyramids are 5.67λ, 3.73λ, 2.75λ, 2.15λ for apex angles 20°, 30°, 40°, 50° respectively. Table 1 shows reflection coefficients in decibel for 2 GHz.

Table 1. Reflection coefficient for different apex angle and incidence angle of pyramidal absorber array. (Urethane %26 loading f=2 GHz L=2λ)

Apex angle											
20°			30°			40°			50°		
H=5,67λ			H=3,73λ			H=2,75λ			H=2,15λ		
Incidence angle	|R| (dB) TE	TM	Incidence angle	|R| (dB) TE	TM	Incidence angle	|R| (dB) TE	TM	Incidence angle	|R| (dB) TE	TM
0°	-48,1	-44	0°	-42,6	-43,2	0°	-32	-32,8	0°	-25,3	-25,5
30°	-64,6	-61,7	30°	-55,5	-62,4	30°	-39,3	-48,7	30°	-27,3	-35,6
60°	-45,6	-40,2	60°	-30,9	-50,1	60°	-36,8	-29,2	60°	-28,9	-24,5

4. Conclusion

Results show that 20° apex angle has better absorption performance than others but it has 5.67λ height and this limits chamber space significantly. 30° apex angle can provide optimal absorption performance based on percentage of height increment. Increment percentage is 35.64% according to 30° apex angle while 20° apex angle's increment percentage is 52.01% and 40° apex angle's increment percentage is 27.91%. For example, for a 10m x 10m rectangular chamber with covered pyramidal absorber arrays, 20° apex angle will occupy 16.29% of total chamber area while 30°, 40° and 50° apex angles occupy 10.88%, 8.08% and 6.35% respectively.

5. References

1. Sedef Kent, Mesut Kartal, "Genetic algorithm approach on pyramidal dielectric absorbers," *International Journal of RF and Microwave Computer-Aided Engineering,* Volume 18 Issue 3 , Pages 286-294, May 2008.

2. W. H. Emerson, "Electromagnetic wave absorbers and anechoic chambers through the years," *IEEE Trans. Antennas Propagat.*, vol. 21, pp. 484–490, 1973.

3. L. K. Neher, “Nonreflecting background for testing microwave equipment,” *US. Patent 2 656 535,* Oct. 20, 1953.

4. C.L. Holloway, R.R. DeLyser, R.F. German, P. McKenna, and M. Kanda, “Comparison of electromagnetic absorber used in anechoic and semi-anechoic chambers for emissions and immunity testing of digital devices,” *IEEE Trans Electromagnetic Compatibility* 39 (1997), 33–47.

5. G. A. Deschamps, “Ray techniques in electromagnetics,” *Proc. IEEE,* vol. 60, pp. 1022-1035, Sept. 1972.

6. David K. Cheng, *Field and Wave Electromagnetics, Second Edition*, Addison Wesley, 1989, pp. 411-417.